EUROPEAN ORGANIZATION FOR NUCLEAR RESEARCH

CERN-PPE/95-120
11 July 1995

LIGHT QUARK SPECTROSCOPY

Alberto Masoni
INFN Sezione di Cagliari
via Ada Negri 18, I-09127 Cagliari Italy
and
CERN, Geneva, Switzerland

ABSTRACT

The main interest in light meson spectroscopy is the search for glueballs. In this field the most recent results concern the scalar ($f_0(1500)$) and pseudoscalar ($E/\iota(1440)$). They are perhaps some of the most promising candidates for being exotics states. New results, coming from $\bar{p}p$ annihilation at rest, with statistics exceeding by an order of magnitude the previous ones, have been recently presented on these states. These results, together with a comparison with the other ones, available from different production processes, will be discussed in this review.

Invited talk at the XV International Conference on Physics in Collision
Cracow, Poland June 8-10 1995
to be published by Ed. Frontières

1. Introduction

The main result expected in light quark spectroscopy is the identification of glueballs or hybrid states. Their existence is one of the foundations of QCD as a non-Abelian field theory. Their unambiguous identification would constitute a striking prove of its validity. Unfortunately despite the existence of such states is foreseen by theory, precise and reliable predictions concerning masses and widths are very difficult. However QCD inspired models as that by Godfrey and Isgur [1] are commonly accepted to describe the $q\bar{q}$ spectrum in the low-mass region. They provide a guide which can be helpful in discriminate ordinary $q\bar{q}$ mesons from exotic states.

We can try to classify exotics (see for example ref. [2]) in the following way:

- exotic states can have exotic quantum numbers (i.e. Q>1 and S>1) not possible for $q\bar{q}$ states (this does not apply to glueballs); they are called exotics of the first kind.
- Glueballs and hybrids can have exotic J^{PC} quantum numbers not accessible to ordinary mesons; they are called exotics of the second kind.
- Mesons are grouped in J^{PC} nonets. QCD models can help in finding the states which best fit in a nonet. Outsiders are candidate for being exotics (exotics of the third kind).

Moreover:

a) Glueballs and hybrids can have anomalous production or decay characteristics.

b) Glueballs are SU(3) singlets, they do not carry either charge or flavors.

c) From point b) it follows that glueballs do not couple directly to photons.

d) Point b) implies also that glueballs are expected to decay 'flavour blind' (taking into account phase space corrections).

e) Glueballs are expected to be copiously produced in 'gluon rich' environments.

The points listed above lead us to an experimental strategy which can allow to disentangle a glueball or an hybrid from a normal $q\bar{q}$ state. Since any exotic state must lay outside SU(3) nonets, a careful spectroscopy study is the basis of any exotic search, to assert the ordinary states in a nonet and distinguish outsiders. Unfortunately this is a very difficult task due to the complexity of the hadron spectrum with the overlap of $q\bar{q}$ ground states and radial excitations. Therefore quality requirements are necessary to accept a state as established. High statistics, good signal-background ratio and confirmation by more than

one experiment are mandatory. Moreover the comparison of results, obtained using different production mechanisms, is a fundamental experimental tool. In particular, from point c) and e) glueball production is expected to be suppressed in $\gamma\gamma$ collision and enhanced in J/ψ decay. J/ψ decay is traditionally considered as a favourite process for glueball production but also antinucleon-nucleon annihilation and hadro-production are good laboratories for glueball studies. Solid evidence for a glueball can come only from a detailed comparison of the results obtained from these different production mechanisms. Following point d) it is evident that also a study of the decay pattern is necessary.

In summary an experimental strategy for exotic searches must rely on a set of high quality and high statistics data, coming from different dynamical sources, which must provide unambiguous spin parity assignments and precise measurements of the decay modes.

Looking at the experimental situation it is evident that a large amount of information is available but we still lack some important elements. Perhaps too many states are present and most of them do not satisfy the quality requirements quoted above.

A detailed discussion of the present experimental situation in exotic searches is beyond the scope of this talk. For a comprehensive review see [3,4].

Here I will restrict myself to the most recent results on the scalar ($f_0(1500)$) and pseudoscalar ($E/\iota(1440)$) sectors. They are perhaps some of the most promising candidates for being exotics states. New results, coming from $\bar{p}p$ annihilation at rest, with statistics exceeding by an order of magnitude the previous ones, have been recently presented on these states. These results, together with a comparison with the other ones, available from different production processes, will be discussed in this review.

2. The $f_0(1500)$

$f_0(1500)$ is I=0 0^{++} state recently presented by Crystal Barrel in their analysis of $\pi^0\pi^0\pi^0$, $\pi^0\pi^0\eta$, and $\pi^0\eta\eta$ final states from $\bar{p}p$ annihilation at rest in liquid hydrogen.

The complexity of the experimental situation concerning this state requires a detailed discussion.

In 1989 a state at a mass of 1565 MeV was discovered by the Asterix experiment in $\bar{p}p$ annihilation at rest on a gaseous hydrogen target [5] (see fig. 1). The state appeared to come mainly from P states of the $\bar{p}p$ atom and the spin parity analysis indicated it was a tensor with quantum numbers 2^{++}.

Again, in $\bar{p}p$ at rest a 2^{++} state was recognized, at 1515 MeV, decaying into

Figure 1: $\pi^+\pi^-$ invariant mass distribution from $\bar{p}p$ annihilation at rest in a gaseous hydrogen target at NTP (a) and in coincidence with X-rays (b) [5]

Also in $\bar{n}p$ annihilation a state at 1502 MeV was identified, in the $\pi^+\pi^-\pi^+$ final state, by the Obelix Collaboration. Spin assignment 2^{++} was found to be the most favourable [7,8].

Crystal Barrel, in the $\pi^0\eta\eta$ final state, identified two scalar resonances, at 1400 and at 1560 MeV, decaying in $\eta\eta$ [9]. The first one was also present in the $\pi^+\pi^-\pi^+\pi^-$ spectrum in the reaction $\bar{n}p \to \pi^+\pi^-\pi^+\pi^-\pi^+$ [8]. The second one was identified as a new resonance. Its mass, width and decay mode resembled the $f_0(1590)$ discovered by GAMS [10]. Suggestions concerning its possible glueball nature were made. Still, the presence of $f_2(1515)$, the tensor previously identified in $\pi^0\pi^0$, was required.

2.1. High statistics data in $\bar{p}p$ annihilation at rest

This situation claimed for further data sample and analyses, to understand the number and the nature of the states present in the 1500 MeV mass region.

From simultaneous analysis of $\pi^0\pi^0\pi^0$ and $\pi^0\eta\eta$ data [11], Crystal Barrel confirmed the presence of two scalar resonances, both in $\eta\eta$ and $\pi^0\pi^0$, with masses and widths $M_1 = 1365$, Γ_1=270 MeV, $M_2 = 1520$, Γ_2=150 MeV.

The main difference, with the previous result, was, of course, that the dominant contribution of the structure at 1500 MeV, decaying in $\pi\pi$, was explained by spin 0 instead of spin 2. This was mainly related to the analysis approach, in which a new parameterization for the $\pi\pi$ S-wave was used and , expecially, $^1S_0$ $\bar{p}p$ annihilation was assumed, not allowing P-states, which were the main source for AX/$f_2(1515)$. The knowledge of the actual contribution of S- and P- states in liquid hydrogen and the relevance of data with a different S- P- mixture, was recognized as very important. The analogy of the $f_0(1500)$ with the G/$f_0(1590)$ motivated the Crystal Barrel collaboration to search for the $f_0(1500)$ decay mode in $\eta\eta'$ in the final state $\pi^0\eta\eta'$. A threshold enhancement (see fig. 2) in the $\eta\eta'$ mass was identified with the $f_0(1500)$ [12]. The obtained mass and width were 1545±25 and 100±40 respectively.

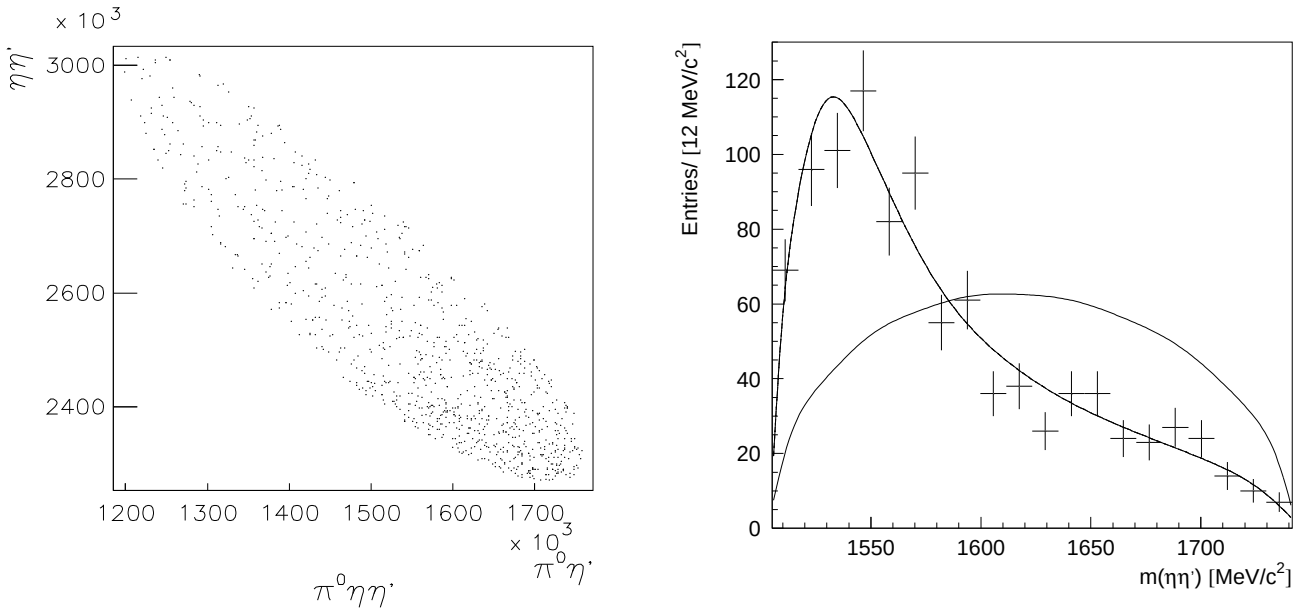

Figure 2: $\bar{p}p$ annihilation at rest in liquid hydrogen. $\pi^0\eta\eta'$ Dalitz Plot (a) and $\eta\eta'$ invariant mass with fit superimposed (b); the pure phase space shape is also shown [12].

In a successive paper [13], results from a very high statistics $\pi^0\pi^0\pi^0$ data sample (712000 events) were presented. The statistics was more than an order of magnitude larger than the sample used in the analyses of ref [6] and allowed to identify with good accuracy two states in the region around 1500 MeV. A scalar state: $f_0(1500)$ and a tensor state: $f_2(1520)$. Results of several fits were reported and again the ambiguity concerning the real contribution of S- and P-states remained. Nevertheless all the fits are in agreement in identifying a scalar resonance at a mass M = 1490±13 MeV and width Γ=120±15 MeV.

The most recent results come from the coupled channel analysis of the three final states: $\pi^0\pi^0\pi^0$ (712000 events), $\pi^0\pi^0\eta$ (280000 events) and $\pi^0\eta\eta$ (198000 events) [14,15].

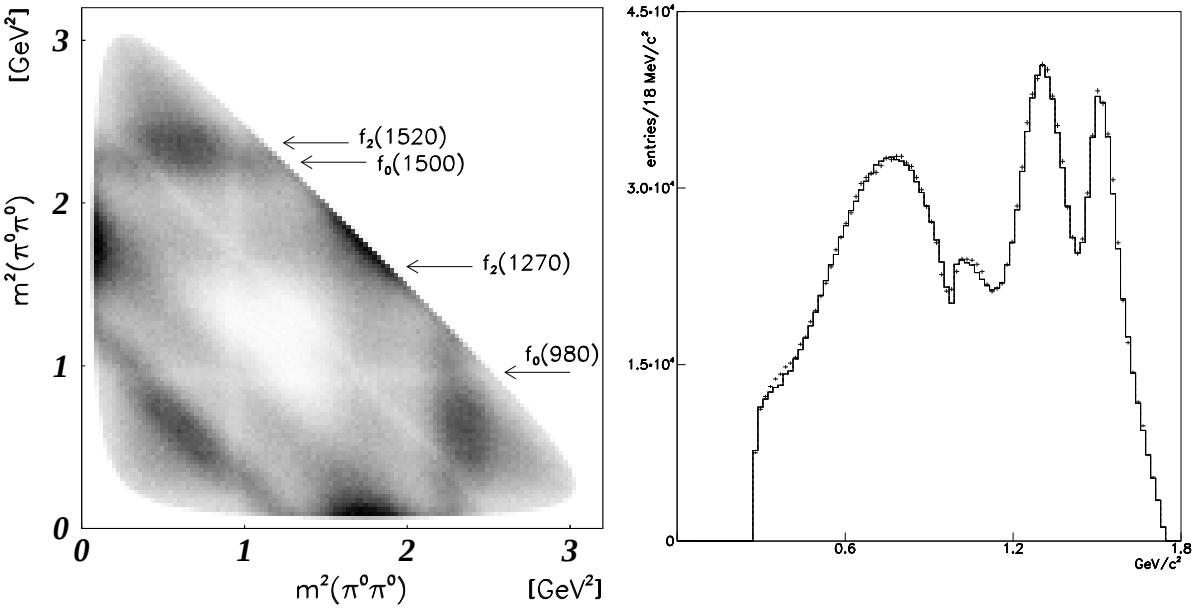

Figure 3: $\bar{p}p$ annihilation at rest in liquid hydrogen. $\pi^0\pi^0\pi^0$ Dalitz Plot (a) and $\pi^0\pi^0$ invariant mass with fit superimposed (b) [13].

The $\pi^0\pi^0\pi^0$ Dalitz plot (fig. 3 a) and the $\pi^0\pi^0$ projection (fig. 3 b) show striking signals of $f_2(1270)$ and $f_0(1500)$. The blob, close to $f_0(1500)$ band, can be interpreted partly as due to the low energy $\pi^0\pi^0$ S-wave and partly as the indication of a tensor structure $f_2(1520)$ which can be the AX(1565) seen originally by Asterix. Its contribution appears to be smaller but this is not surprising. AX(1565) was recognized coming from the P- states of the $\bar{p}p$ atom in annihilation at rest in gaseous hydrogen [5]. In liquid hydrogen S-wave dominance is assumed according to the well accepted Day-Snow-Sucher mechanism [16]. Actually the data can be described using $^1S_0$ only as initial state [11,13] even if the fit improves allowing for P states contribution. However an unexpected substantial P- wave contribution is obtained in this case (up to 50%).

An independent determination of the six J^{PC} fractions could be extremely useful, in solving this problem and disentangling the scalar and the tensor contributions. A clarification is expected from data taken with different $\bar{p}p$ initial angular momentum states distribution using a gaseous target [13]. Nevertheless it is important to notice that all the fits require the contribution of the $f_0(1500)$, regardless the initial state distribution.

The $\pi^0\eta\eta$ Dalitz plot (fig. 4 a) is dominated by the interference at center of the two $a_0(980)$ bands with a $\eta\eta$ band at 1500 MeV. In this structure again a scalar and a tensor state are required. The 0^{++} has mass (1505 ± 15) and width (120 ± 30) the 2^{++} has mass (1530 ± 15) but the width is uncertain. An additional $\eta\eta$ intensity is identified as $f_0(1370)$. The $f_0(1370)$ and $f_0(1500)$ are identified in the $\eta\eta$ projection (fig. 4 b) while the $\eta\pi^0$ projection shows a clear a_0 signal (fig. 4 c).

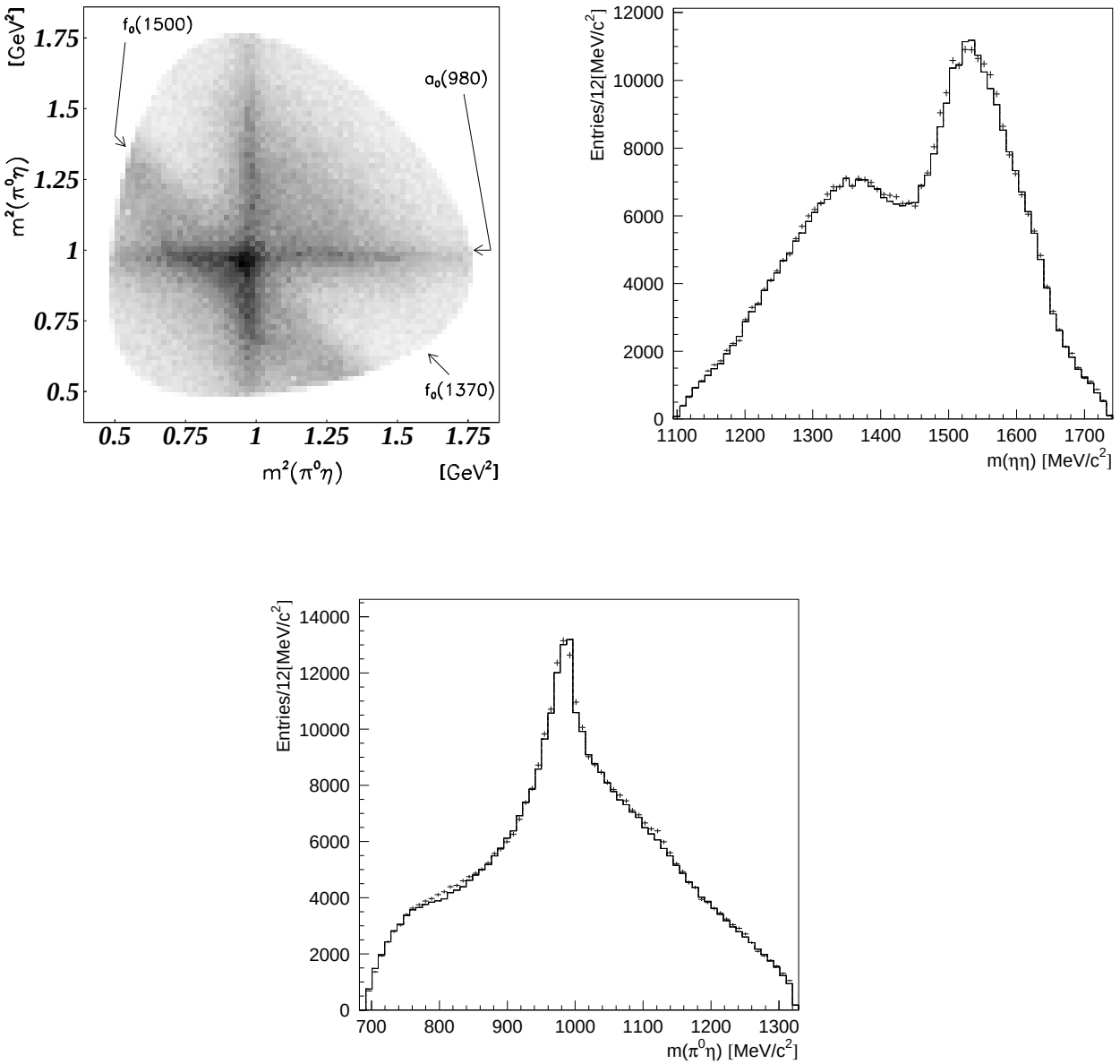

Figure 4: $\bar{p}p$ annihilation at rest in liquid hydrogen. $\pi^0\eta\eta$ Dalitz Plot (a), $\eta\eta$ invariant mass with fit superimposed (b), $\eta\pi^0$ invariant mass with fit superimposed (c) [13].

In the $\pi^0\pi^0\eta$ Dalitz plot (fig. 5) the $a_0(980)$, the $f_0(980)$ and the $a_2(1320)$ are clearly evident. Moreover the presence of a new isovector scalar resonance $a_0(1450)$ is required to satisfactory describe the data.

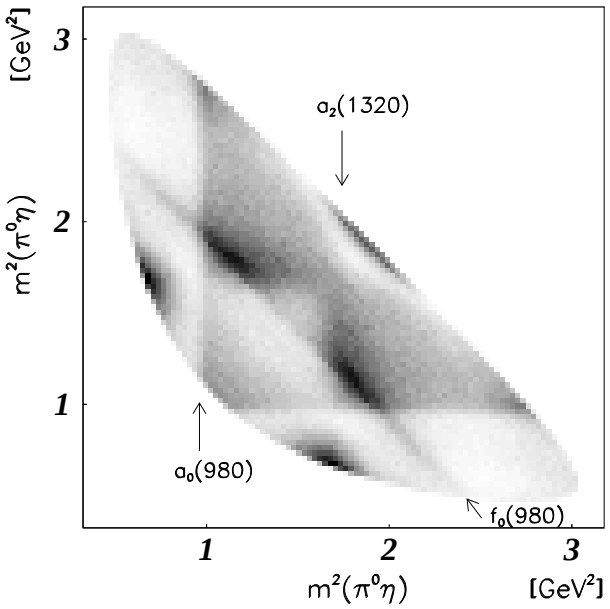

Figure 5: $\bar{p}p$ annihilation at rest in liquid hydrogen. $\pi^0\pi^0\eta$ Dalitz Plot [13].

The coupled channel analysis is based on a 3 x 3 K-matrix incorporating the $\pi\pi$, $K\bar{K}$ and $\eta\eta$ channels. In the fit S-wave dominance was assumed and contributions from P-states were neglected. The fit provides simultaneous description of the three final states mentioned above, together with the $\pi\pi$ scattering data of ref. [17,18]. The fit confirms essentially the results obtained by the analysis of each Dalitz plot.

From the fit the couplings of $f_0(1500)$ to $\pi^0\pi^0$ and $\eta\eta$ were extracted. Comparing them to the measurement of the decay mode in $\eta\eta'$ [12] and to the results which can be extracted from bubble chamber data for $K\bar{K}$ [19] one obtains:

$$\pi\pi : \eta\eta : \eta\eta' : K\bar{K} = 3 : 0.70\pm0.27 : 1.00\pm0.46 : < 0.4$$

2.2. Other experimental results

Before discussing the implications of these results, concerning the nature of $f_0(1500)$, on the basis of the points discussed in the introduction, it is worthwhile an attempt to compare these data with the other results available from other production mechanisms and final states.

2.2.1. $\bar{p}p$ annihilation in flight

The final states $\pi^0\pi^0\pi^0$ and $\pi^0\eta\eta$ have been studied in $\bar{p}p$ annihilation in flight by the E760 experiment at Fermilab at 3 GeV/c incident $\bar{p}$ momentum. Both the $\pi^0\pi^0\pi^0$ and the $\pi^0\eta\eta$ Dalitz plots show clear evidence for a resonance at 1500 MeV decaying in $\pi^0\pi^0$ and $\eta\eta$ (see fig. 6). From the preliminary spin parity analysis [20] a 2^{++} state is required. The introduction of a 0^{++} state at the same mass slightly improves the fit.

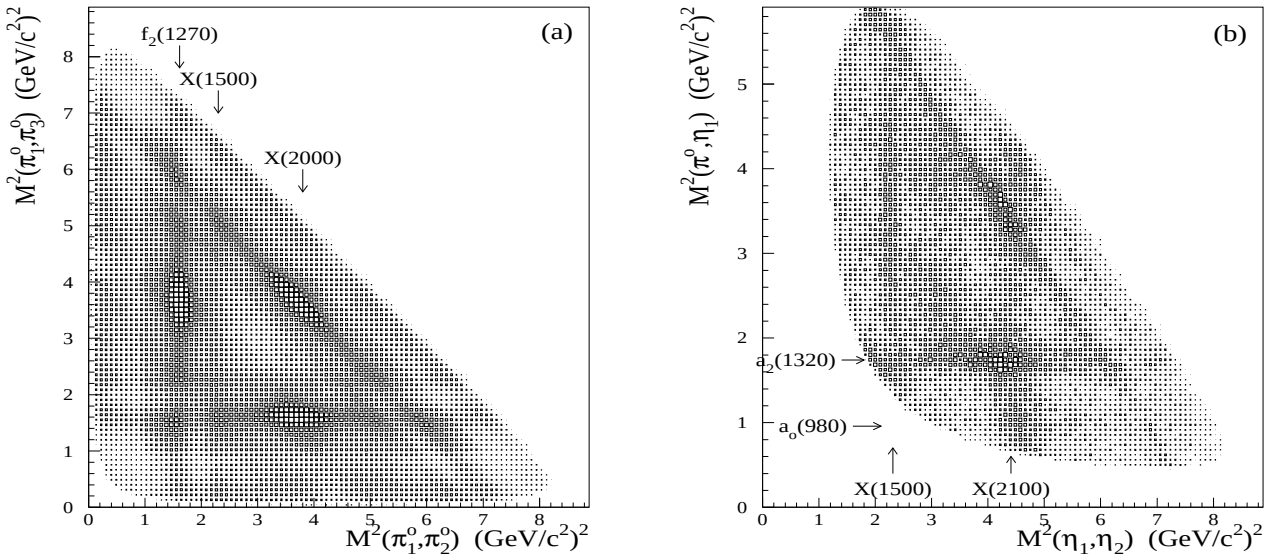

Figure 6: $\bar{p}p$ annihilation at 3 GeV/c incident $\bar{p}$ momentum. Dalitz Plots for $\pi^0\pi^0\pi^0$ (a) and $\pi^0\eta\eta$ [20].

Also Crystal Barrel has given some preliminary results from $\bar{p}p$ annihilation in flight at 1940 MeV/c incident $\bar{p}$ momentum [21]. At this energy the signal of $f_0(1500)$ is shrinked into the middle of the $\pi^0\pi^0\pi^0$ Dalitz plot (fig. 7 a). A hint of its presence is perhaps present but it is not possible, at this stage, to extract firm conclusions. The signal weakness is surprising since it is well evident both in the data at rest of Crystal Barrel and in the data in flight of E760. On the contrary a well defined narrow signal at 1500 MeV is present in the $\pi^0\eta\eta$ final state (fig. 7 b,c). Spin parity analysis on these data is currently in progress.

Figure 7: $\bar{p}p$ annihilation at 1940 MeV/c incident $\bar{p}$ momentum. $\pi^0\pi^0\pi^0$ Dalitz Plot (a) $\pi^0\eta\eta$ Dalitz Plot (b), $\eta\eta$ invariant mass (c).

2.2.2. $\bar{n}p \to \pi^+\pi^-\pi^+$, $\bar{n}p \to \pi^+\pi^-\pi^+\pi^-\pi^+$, $\bar{p}p \to \pi^+\pi^-\pi^0$

The $\pi^+\pi^-\pi^+$ and $\pi^+\pi^-\pi^+\pi^-\pi^+$ final states have been studied by the Obelix experiment under different initial angular momentum and isospin conditions. The data on $\bar{n}p$ annihilation in 3 and 5 charged pions allow to select I=1 initial state. The latest results on the $\pi^+\pi^-\pi^+$ final state [22] (fig. 8) indicate that probably two states, a 0^{++} at 1540±15 MeV, $\Gamma = 155 \pm 15$ MeV and a 2^{++} at 1565±20 MeV, $\Gamma = 135 \pm 15$ MeV, are present. The broad scalar resonance at 1350 MeV is confirmed by the analysis of the $\pi^+\pi^-\pi^+\pi^-\pi^+$ final state [22].

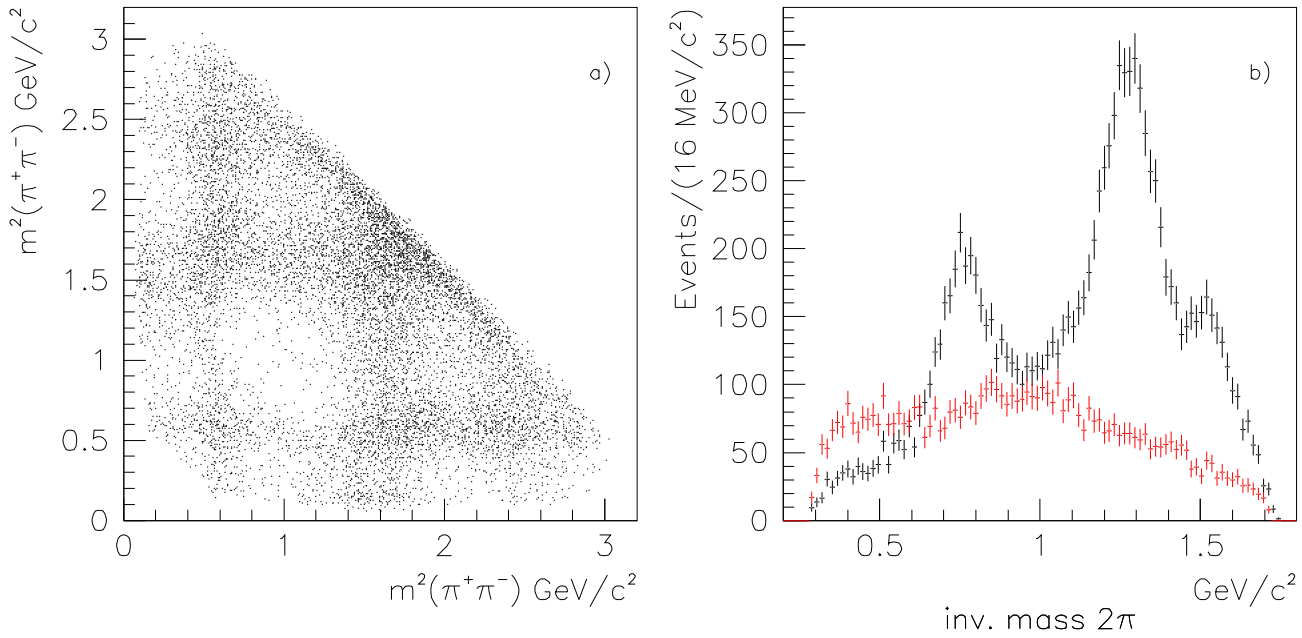

Figure 8: $\bar{n}p$ annihilation at 400 MeV/c incident $\bar{n}$ momentum. $\pi^+\pi^-\pi^+$ Dalitz Plot (a) and $\pi^+\pi^-$ invariant mass (b) [22].

Data on $\bar{p}p$ annihilation at rest with different target densities (hence different initial angular momentum states distribution) have been taken for the final state $\pi^+\pi^-\pi^0$. With respect to the 3 π^0 final state the situation is more complicated due to interference effects of the ρ. The preliminary results [23] of the simultaneous fit of two data samples, low pressure (P-wave dominant) and NTP (about the same fraction of S and P-wave), indicate, in the 1500 MeV mass region, the simultaneous presence of two states, a scalar and a tensor [23]. The scalar appear produced totally from $^1S_0$ $\bar{p}p$ state while the tensor comes dominantly from the $^3P_2$ state.

2.2.3. Central production

The presence of a scalar resonance has been reported in central production by the WA91 experiment [24] in the reaction pp$\rightarrow$ $p_f(\pi^+\pi^-\pi^+\pi^-)p_s$ at 450 GeV/c (see fig. 9 a,b). The mass was 1450 MeV and its evidence in a *gluon rich* environment made it an interesting glueball candidate. More recent results from WA91 collaboration [25] show evidence for a scalar state decaying also in $(\pi^+\pi^-)$ (see fig. 9 c,d) compatible with the $f_0(1500)$ of Crystal Barrel (M = 1497$\pm$30 MeV and $\Gamma = 199 \pm 30$ MeV). Moreover another interpretation of the state at 1450 decaying in 4π is discussed. In this interpretation the peak at 1450 can be the result of interference of $f_0(1370)$ and $f_0(1500)$. The same should apply to the state decaying in two pions but there the contribution of $f_0(1370)$ looks very small.

Figure 9: pp$\rightarrow p_f(\pi^+\pi^-\pi^+\pi^-)p_s$ at 450 GeV/c. $\pi^+\pi^-\pi^+\pi^-$ invariant mass for the full data sample (a) and for $\mid t_1 \mid \leq 0.15(GeV)^2$ and $\mid t_2 \mid \leq 0.15(GeV)^2$ (b); $\pi^+\pi^-$ invariant mass fitted with $f_0(1500)$ (c) and with $f_0(1450)$ (d) [25].

2.2.4. J/ψ decay

It is natural now to look at the *natural hunting field* for glueballs, namely the J/ψ decays. Results from Mark III and DM2 on J/$\psi \rightarrow \gamma(\pi^+\pi^-\pi^+\pi^-)$ show evidence of a a peak in the 4π mass around 1500 MeV. The old DM2 analysis [26] showed that the structures present in their spectrum are due to 0^{-+} resonances. Recent results, from a new analysis of Mark III data [27], have shown that also in the 4π channel a 0^{++} signal at 1505 MeV is present see fig. 10). One of the main features of the new analysis is the inclusion of the $\pi\pi$ S-wave (σ) as in Crystal Barrel analysis. The fit returns a sizable 0^{++} contribution from $f_0(1500)$ decaying in $\sigma\sigma$.

Figure 10: $J/\psi \to \gamma(\pi^+\pi^-\pi^+\pi^-)$. $\pi^+\pi^-\pi^+\pi^-$ invariant mass, fit with $f_0(1500)$ (a) and without $f_0(1500)$ (b) [27].

One may remark the absence of $f_0(1500)$ in $J/\psi \to \gamma(\pi^+\pi^-)$. However, even if no firm conclusion from the data is available at the moment, it is possible that the decay ratio $4\pi/2\pi$ could be definitely larger than 1. The small statistics on $J/\psi \to \gamma(\pi^+\pi^-)$ could be not sufficient to obtain evidence for the signal.

2.2.5. The $G/f_0(1590)$

A 0^{++} state was reported, at 1590 MeV, about ten years ago, by the GAMS experiment in the analysis of $\pi^- p \to \eta\eta n$ at 100 GeV/c [28,29] (see fig. 11).

Figure 11: $\pi^- p \to \eta\eta n$ at 100 GeV/c. $\eta\eta$ invariant mass [29].

The $G/f_0(1590)$ is a long standing candidate for being the scalar glueball. GAMS identified it in $\eta\eta$ and $\eta\eta'$ decay modes [10]. What was surprising was the large coupling to $\eta\eta'$ with respect to $\eta\eta$ (2.7 ± 0.8). This was interpreted as evidence for its exotic nature [30].

It can be the same state as $f_0(1500)$ but remains to explain the differences with Crystal Barrel in the $\eta\eta'$ and $\pi^0\pi^0$ decay modes (besides the differences in mass and width).

2.3. Summary of the experimental situation

One can try to sum up the experimental situation as follows.
The presence of a scalar resonance around 1500 MeV is reported in:

- $\bar{p}p$ annihilation at rest in liquid hydrogen $(\pi^0\pi^0, \eta\eta, \eta\eta')$[12,13]
- $\bar{n}p$ annihilation $(\pi^+\pi^-)$ [22]
- $\bar{p}p$ annihilation $(\pi^+\pi^-)$ [23]
- central production $(\pi^+\pi^-\pi^+\pi^-, \pi^+\pi^-)$ [25]
- J/ψ decay $(\pi^+\pi^-\pi^+\pi^-)$ [27]
- $\pi^- p \to \eta\eta n$ at 100 GeV/c $(\eta\eta, \eta\eta')$ [29]

The presence of a 2^{++} resonance is reported in $\bar{p}p$ annihilation in flight $(\pi^0\pi^0, \eta\eta)$ [20].

Simultaneous evidence of the presence of a scalar and a tensor in the 1500 MeV region is reported in:

- $\bar{p}p$ annihilation at rest in liquid hydrogen $(\pi^0\pi^0, \eta\eta, \eta\eta')$[12,13]
- $\bar{p}p$ annihilation $(\pi^+\pi^-)$ [23] (not well established)
- $\bar{p}p$ annihilation in flight $(\pi^0\pi^0, \eta\eta)$ [20] (not well established)

Some inconsistencies are present:

- If G(1590) and $f_0(1500)$ are the same object the GAMS and the Crystal Barrel data are not consistent in their measurements of the $\pi^0\pi^0$ and $\eta\eta'$ decay modes.
- It is not clear why the signal disappears in Crystal Barrel data in flight in $\pi^0\pi^0$ if it is so strong, in the same channel, in E760 data.
- It is also not clear why, in $\bar{n}p \to \pi^+\pi^-\pi^+\pi^-\pi^+$, there are no hints of the $f_0(1500)$ signal (which is reported by J/ψ decay and central production data in the same final state).

In conclusions, as shown above, the presence of a 0^{++} resonance at 1500 MeV appears well asserted by data from many production mechanisms and in many decay modes .

New data, to study its coupling to $K\bar{K}$ are mandatory.

It is also still to clarify the contribution of the 2^{++} state. For this, high statistics data, under different initial state conditions are necessary.

2.4. The nature of $f_0(1500)$

Since its discovery $f_0(1500)$ was proposed as a candidate for being a glueball. The amount of data now available allow to reinforce this hypothesis [31]. It is found in production processes where glueball production are traditionally expected to be enhanced (central production and J/ψ decay). The great amount of data coming from $\bar{p}p$ annihilation confirms that this process also can favour glueballs formation.

The data for the different decay modes [13,14] do not fit the $q\bar{q}$ hypothesis [31]. Unfortunately the finite $\eta\eta'$ decay mode and the apparent suppression of $K\bar{K}$ decay disagrees also from what expected from flavour blindness for a glueball state. Mechanisms [14,31] are suggested to explain the decay pattern modification.

Evidence for the non $q\bar{q}$ nature of $f_0(1500)$ come also from the study of the scalar nonet. Table I lists the known scalar mesons. We tentative assume $f_0(1500)$ and G/$f_0(1590)$ as being the same state.

I = 0	I = 1	I = 1/2
$f_0(980)$	$a_0(980)$	$K_0^*(1430)$
$f_0(1400)$	$a_0(1450)$	
$f_0'(1525)$		
$f_0(1500)$		

Table 1. The known 0^{++} states

The nature of $a_0(980)$ and $f_0(980)$ has long being discussed. Their masses, very far from the Godfrey-Isgur model predictions [1] and their strong $K\bar{K}$ coupling supported the hypothesis of being both $K\bar{K}$ molecules [32]. However the analysis of Morgan and Pennington [33] on J/ψ decay, central production and elastic $\pi\pi$ and $K\bar{K}$ scattering, gives clear preference to the standard resonance hypothesis for both states.

Also Törnqvist, in a recent paper [34] includes $a_0(980)$ and $f_0(980)$ as members of the 0^{++} nonet.

Despite some discrepancies that still exists in decay modes and the need for further confirmation for $a_0(1450)$ and $f_0'(1525)$, there is a good indication that

$f_0(1500)$ can be identified as an extra state in the nonet.

Moreover the mass of $f_0(1500)$ is in reasonable agreement with expectations for the lightest scalar glueball from lattice calculations [35,36,37].

In conclusions we might say that, unfortunately, nature has not provided us unambiguous signatures in identifying $f_0(1500)$ as a scalar glueball. Nevertheless many experimental data are available and their analysis strongly favour its interpretation as a non $q\bar{q}$ state. In particular more constraints could be put when new data concerning its $K\bar{K}$ coupling will be available [31].

3. The E/ι

Historically the E/ι represented the first gluonium candidate since the observation by the Mark II[38] and Crystal Ball[39] experiments of a large signal at 1440 MeV in the J/ψ radiative decay $J/\psi \to \gamma K\bar{K}\pi$.

Figure 12: J/$\psi \to \gamma(K\bar{K}\pi)$. $K\bar{K}\pi$ invariant mass (a) Decay Dalitz plot for M$(K\bar{K}\pi) > 1410$ MeV (b) and for M$(K\bar{K}\pi) > 1410$ MeV (c) [41].

The first discovery of the E/ι signal actually dates back to 1963[40], in $\bar{p}p$ annihilation at rest. After more than 30 years, despite the great number of experiments, the number and the nature of the objects present in the 1400 - 1500 MeV mass region is not yet clarified.

Inconsistencies are present in the number of resonances, in their spin assignments and decay modes even within experiments which studied the same final state from the same production mechanism (for a detailed review of the subject see ref. [43,4].

Despite this rather confuse situation it appears that a dependence from the dynamical source is present. The axial vector is clearly seen in hadroproduction and J/ψ decay in the $K\bar{K}\pi$ final state. It is apparently not present in $\bar{p}p$ at rest (perhaps it is present in flight [44]) neither is seen in the $\eta\pi\pi$ decay mode.

On the contrary a pseudoscalar is seen in almost all final states and production mechanisms except for $\gamma\gamma$ collision and central production.

The data on J/ψ radiative decay[41,42] claim for the presence of three objects: two pseudoscalars and an axial vector. This is the only case in which three states have been identified within the same data set. In fig. 12 the data from the Mark III experiment [41] are shown.

3.1. $E/\iota \to K\bar{K}\pi$ from $\bar{p}p$ annihilation at rest

Since the first bubble chamber measurement (1963) only two other experiments investigated $E/\iota \to K\bar{K}\pi$ on $\bar{p}p$ annihilation at rest.

The Asterix experiment [45] took data with a gaseous hydrogen target. The statistics was not sufficient for a spin parity analysis but from comparison of the branching ratio measured at NTP and the bubble chamber results in liquid hydrogen [40] the 0^{-+} assignment was inferred.

Actually, in $\bar{p}p \to E/\iota(\pi\pi)$, being $M_{E/\iota}$ much greater than the dipion mass, the $(\pi\pi)$ system is in S-wave and the relative angular momentum L is also equal to zero. Therefore, a 0^{-+} resonance comes mainly from a $^1S_0$ $\bar{p}p$ state and a 1^{++} resonance from a $^3P_1$ $\bar{p}p$ state. This is a unique feature of $\bar{p}p$ at rest and results in a powerful tool to disentangle states close in mass but with different spin by performing a selection of the initial angular momentum state. Moreover it allows to take indications concerning the nature of the state(s) present on the basis, not only of spin parity analysis, but also from comparison of annihilation frequencies from different initial state conditions (as in the case of Asterix).

Very recently the Obelix collaboration has presented the results from a high statistics data sample taken with a liquid hydrogen target (about 18 million 4 prong events with a charged kaon trigger) [46]. The $K\bar{K}\pi$ invariant mass spectrum is shown in fig. 13.

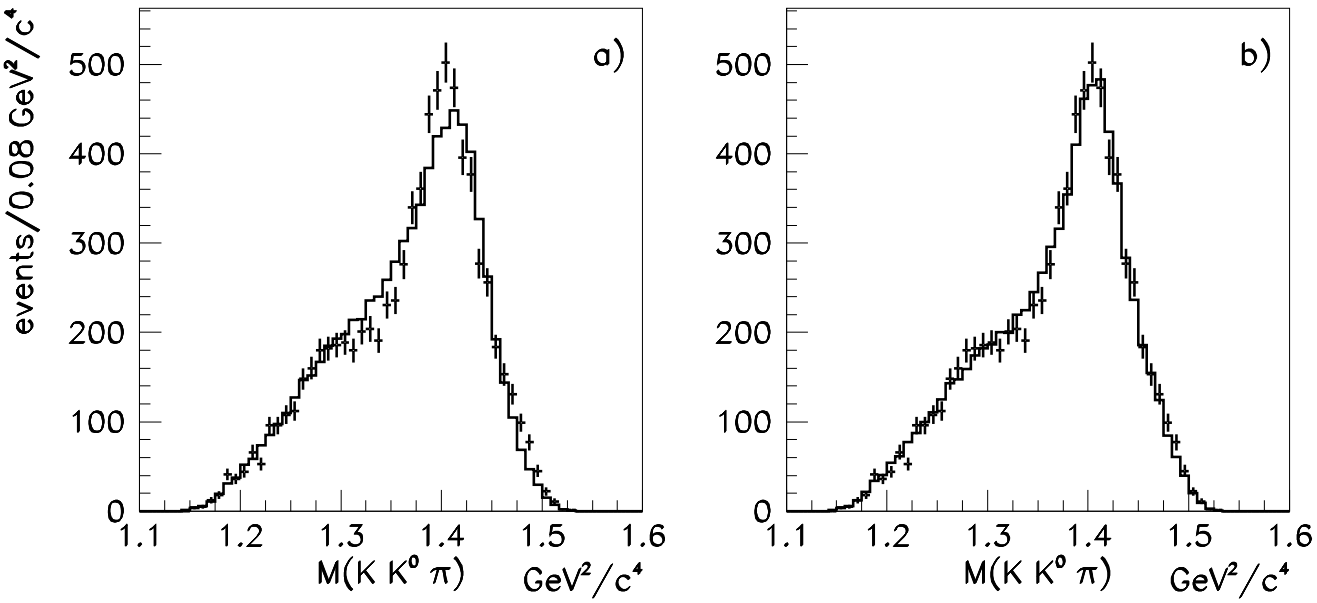

Figure 13: $\bar{p}p$ annihilation at rest in liquid hydrogen. $K\bar{K}\pi$ invariant mass with fit for the one 0^{-+} (a) and two 0^{-+} (b) hypotheses (2 entries per event) [46].

The preliminary results of the spin parity analysis of 4000 E/ι decays in the $K\bar{K}\pi$ channel confirm the presence of two pseudoscalars: the first one with mass $M_1 = 1410$ MeV and a width $\Gamma_1 = 70$ MeV decaying dominantly in $a_0\pi$; the second one with mass M_2=1500 MeV and a width Γ_2=240 MeV, which decays dominantly to K*K.

The indication of a 1^{++} is very weak and compatible with 0. This latest result is not conclusive, concerning the presence of an axial vector in $\bar{p}p$ at rest since, in liquid hydrogen, annihilation from $\bar{p}p$ P states is expected to be very small due to the Day Snow Sucher [16] mechanism. The approach followed by Obelix [47,48] is to obtain a selection of the initial angular momentum state by employing targets at different pressures thanks to the dependence of S- and P-wave fractions (and their six hyperfine levels) from the gas density. In practice it is possible to range from:

i) a situation of S- wave dominance (in liquid hydrogen)

ii) an equal mixture of S- and P- wave (at NTP)

iii) P-wave dominance (at low pressures as few mbar).

The preliminary results show a suppression of about a factor 6 from liquid hydrogen to 5 mbar [46]. This result indicates a dominance of the 0^{-+} state with respect to 1^{++} and gives further confirmation of the validity of the assumption, explained before, according to which a 0^{-+} state comes from a $^1S_0$ $\bar{p}p$ state while a 1^{++} state proceeds from a $^3P_1$ $\bar{p}p$ state.

A high statistics data sample, collected at NTP, will allow a study of the possible presence of the 1^{++} in $\bar{p}p$ annihilation at rest.

3.2. $E/\iota \to \eta\pi\pi$ from $\bar{p}p$ annihilation at rest

No data in this channel were available from $\bar{p}p$ annihilation at rest before the results recently presented by Crystal Barrel [49] on the $4\pi\eta$ final state.

Figure 14: $\bar{p}p$ annihilation at rest in liquid hydrogen. Scatter plots of $\pi\pi\eta$ invariant mass versus recoiling $\pi\pi$ mass (a,b); $\pi\pi\eta$ invariant mass for $M(\pi\pi) <$ 520 MeV (insets) [49].

From these data about 5000 $E/\iota \to \eta\pi^+\pi^-$ and 5000 $E/\iota \to \eta\pi^0\pi^0$ have been identified. Fig. 15 a,b show the scatterplots $M(\pi\pi\eta)$ versus recoiling $M(\pi\pi)$. The accumulation of events in the E/ι region can be easily seen. In fig. 15 (insets) the $\pi\pi\eta$ invariant mass, for the region $M(\pi\pi) < 520$ MeV is shown.

The preliminary results of the spin parity analysis indicate the presence of a 0^{-+} resonance with mass 1410 Mev and with 60 MeV, in agreement with the other results for the lower mass pseudoscalar. This state appears to decay into $a_0\pi$ and $\eta(\pi\pi)_{S-wave}$.

The contribution of a 1^{++} (if present) looks very weak.

3.3. Summary

The confirmation of the presence of two pseudoscalars reinforce the hypothesis of the possible exotic nature of one of them. The object at lower mass, the $\eta(1410)$, in the PDG notation, has long being glueball candidate [3,4]. Its copious production in the traditional *gluon rich* environment (J/ψ decay), together

with the non observation in $\gamma\gamma$, indicate a large gluon content. Also flavour blindness appears to be satisfied by the data.

The MIT bag model [50] predicts a 0^{-+} glueball at a mass around 1400 MeV but it predicts also the scalar glueball at 1000 MeV. More recent lattice calculations [35] moved the scalar glueball to 1500 MeV and the 0^{-+} above 2000 MeV but mixing with $q\bar{q}$ can distort and reorder the glueball spectrum [31,14].

4. Perspectives

One of the main points which deserves further investigation is the decay mode of $f_0(1500)$ to $K\bar{K}$. Up to now only a bubble chamber measurement is available. As underlined in ref. [31] a confirmation of the suppression of the $K\bar{K}$ decay of $f_0(1500)$ will give an important experimental input in the attempt to discriminate the non $q\bar{q}$ nature of this state.

Meson spectroscopy selecting different initial state by means of suitable target system has been already a characteristic feature of the Obelix experimental strategy and it is being pursued in the E/ι study.

Recently also the Crystal Barrel experiment has inserted in its plans [13] measurements with a gaseous hydrogen target in order to solve ambiguities in the fits related to the S/P wave fraction.

5. Conclusions

Concerning the study of $f_0(1500)$ an impressive set of new results have been presented in these latest months from $\bar{p}p$ annihilation, J/ψ decay and central production. They have shown that the complexity of the hadron spectrum makes glueball and hybrids search an extremely difficult task, even in presence of so many high quality results. Nevertheless the available data provide a strong indications in favour of the non $\bar{q}q$ nature of this object and make it a candidate for being the scalar glueball [31].

The study of the long standing E/ι *puzzle* has received a *boost*, this year, with new high statistics data from $\bar{p}p$ annihilation at rest.

The confirmation of the presence of two pseudoscalar objects in the 1400 - 1500 MeV mass region is the main outcome of these data. This result support the hypothesis of the exotic nature for at least one of them.

The results obtained from very high statistics data samples in $\bar{p}p$ annihilation confirm that, besides the traditional environments (J/ψ decay and central production) also $\bar{p}p$ annihilation at rest is a suitable laboratory to exploit, with very high statistics, the search for gluon rich states.

6. Acknowledgments

I want to thank the organizers of the 95 Physics in Collision Conference for their invitation to speak and their warm hospitality in Cracow.

I am grateful to D. Bugg, A. Filippi, A. Hasan, A. Kirk, J. Lüdemann and S. Spanier for the presentation of their experiments results. I want to thank also my colleagues in Cagliari University for fruitful discussions and comments. My deep thanks to C. Guaraldo, L. Montanet and S. Spanier for their valuable suggestions and contributions.

7. References

1. S. Godfrey e N.Isgur, Phys. Rev. D32 (1985) 189.
2. F. Close, Rep. Progr. Phys. 51 (1988) 833.
3. M. Doser and A. Palano, Proc. III Workshop on a τ-charm factory (1993), Bari - TH/171-94.
4. A. Palano, Proc. QCD 94, Montpellier, France July 1994.
5. B. May et al., Phys. Lett. B 225 (1989) 450.
6. E. Aker et al., Phys Lett. B 260 (1991) 249.
7. A. Adamo et al., Phys. Lett. B 285 (1992) 15.
8. A. Adamo et al., Nucl. Phys. A 558 (1993) 13c.
9. C. Amsler et al., Phys. Lett. B 291 (1992) 347.
10. D. Alde et al.,Phys. Lett. B 201 (1988) 160.
11. V.V. Anisovich et al., Phys. Lett. B 323 (1994) 233.
12. C. Amsler et al., Phys. Lett. B 340 (1994) 259.
13. C. Amsler et al., Phys. Lett. B 342 (1995) 433.
14. S. Spanier Proc. Leap 94 Conf., Bled, Slovenia (1994).
15. C. Amsler et al., to be published on Phys. Lett. B.
16. T.B. Day, G.A. Snow e J. Sucher Phys. Rev. Lett. 3 (1959) 61.
17. L. Rosselet et al., Phys. Rev. D 15 (1977) 574.
18. G. Grayer et al., Nucl. Phys. B 75 (1974) 189.
19. L. Gray Phys. Rev. D 27 (1983) 307.
20. M.A. Hasan et al., Proc. Leap '94 Conf., Bled, Slovenia (1994).
21. J. Lüdemann et al., Proc. Leap '94 Conf., Bled, Slovenia (1994).
22. A. Filippi et al., Proc. Leap '94 Conf., Bled, Slovenia (1994).
23. N. Semprini et al., Proc. Leap '94 Conf., Bled, Slovenia (1994).
24. S. Abasitz et al., Phys. Lett. B 324 (1994) 509.
25. F. Antinori et al., Cern/PPE 95-33.
26. D. Bisello et al., Phys. Rev. D 39 (1989) 701.

27. D.V. Bugg et al., Phys. Lett. B, to be published.
28. F. Binon et al., Nuovo Cimento 80 A (1984) 363.
29. D. Alde et al., Nucl. Phys. B239 (1986) 485.
30. S.S. Gershstein et al. Z. Phys. C 24 (1984) 305.
31. C. Amsler and F. Close Phys. Lett. B, to be published.
32. J. Weinstein and N. Isgur Phys. Rev. Lett. D 48 (1982) 659.
33. D. Morgan and M.R. Pennington Phys. Rev. D 48 (1993) 1185.
34. N.A. Törnqvist Z. Phys., to be published.
35. G. Bali et al., Phys. Lett. B 309 (1993) 378.
36. D. Weingarten, Nucl. Phys. B 34 (1994) 29c.
37. J. Wosiek, this Proceedings.
38. D.L. Scharre et al., Phys. Lett. B 97 (1980) 329.
39. C. Edwards et al., Phys. Rev. Lett. 49 (1982) 259.
40. R. Armenteros et al., Proc. of the Siena International Conference on Elementary Particles, vol.1 (1963) 287.
    P. Baillon et al., Nuovo Cim. 3 (1967) 393
41. Z. Bai et al., Phys. Rev. Lett. 65 (1990) 2507.
42. J.E. Augustin et al., Phys. Rev. D 46 (1992) 1951.
43. A. Zenoni, At the Frontiers of Hadronic Physics, World Scient. (1994) 357.
44. V. Vuillemin et al., Lett. Nuovo Cimento 5 (1975) 165.
45. K.D. Duch et al., Z. Phys. C 45(1989) 223.
46. A. Masoni et al., Proc. Leap '94 Conf., Bled, Slovenia (1994).
47. E. Lodi Rizzini Riv. Nuovo Cim. 15 (1992).
48. A. Masoni et al., Nuovo Cimento 107 A 11 (1994) 2279.
49. D. Urner et al., Proc. Leap '94 Conf., Bled, Slovenia (1994).
50. C.E. Carlson, T.H. Hansson and C. Peterson, Phys. Rev. D30 (1984) 1594.

Figure Captions

1) $\pi^+\pi^-$ invariant mass distribution from $\bar{p}p$ annihilation at rest in a gaseous hydrogen target at NTP (a) and in coincidence with X-rays (b) [5]

2) $\bar{p}p$ annihilation at rest in liquid hydrogen. $\pi^0\eta\eta'$ Dalitz Plot (a) and $\eta\eta'$ invariant mass with fit superimposed (b); the pure phase space shape is also shown [12].

3) $\bar{p}p$ annihilation at rest in liquid hydrogen. $\pi^0\pi^0\pi^0$ Dalitz Plot (a) and $\pi^0\pi^0$ invariant mass with fit superimposed (b) [13].

4) $\bar{p}p$ annihilation at rest in liquid hydrogen. $\pi^0\eta\eta$ Dalitz Plot (a), $\eta\eta$ invariant mass with fit superimposed (b), $\eta\pi^0$ invariant mass with fit superimposed (c) [13].

5) $\bar{p}p$ annihilation at rest in liquid hydrogen. $\pi^0\pi^0\eta$ Dalitz Plot [13].

6) $\bar{p}p$ annihilation at 3 GeV/c incident $\bar{p}$ momentum. Dalitz Plots for $\pi^0\pi^0\pi^0$ (a) and $\pi^0\eta\eta$ [20].

7) $\bar{p}p$ annihilation at 1940 MeV/c incident $\bar{p}$ momentum. $\pi^0\pi^0$ invariant mass (a), $\pi^0\pi^0\pi^0$ Dalitz Plot (b) $\pi^0\eta\eta$ Dalitz Plot (c), $\eta\eta$ invariant mass (d) .

8) $\bar{n}p$ annihilation at 400 MeV/c incident $\bar{n}$ momentum. $\pi^+\pi^-\pi^+$ Dalitz Plot (a) and $\pi^+\pi^-$ invariant mass (b) [22].

9) pp$\rightarrow p_f(\pi^+\pi^-\pi^+\pi^-)p_s$ at 450 GeV/c. $\pi^+\pi^-\pi^+\pi^-$ invariant mass for the full data sample (a) and for $\mid t_1 \mid \leq 0.15(GeV)^2$ and $\mid t_2 \mid \leq 0.15(GeV)^2$ (b); $\pi^+\pi^-$ invariant mass fitted with $f_0(1500)$ (c) and with $f_0(1450)$ (d) [25].

10) J/$\psi \rightarrow \gamma(\pi^+\pi^-\pi^+\pi^-)$. $\pi^+\pi^-\pi^+\pi^-$ invariant mass, fit with $f_0(1500)$ (a) and without $f_0(1500)$ (b) [27].

11) $\pi^- p \rightarrow \eta\eta n$ at 100 GeV/c. $\eta\eta$ invariant mass [29].

12) $\bar{p}p$ annihilation at rest in liquid hydrogen. Decay Dalitz plot for M($K\bar{K}\pi$) > 1380 MeV (a), $K\bar{K}\pi$ invariant mass after double charged combination subtraction (b) [40].

13) J/$\psi \rightarrow \gamma(K\bar{K}\pi)$. $K\bar{K}\pi$ invariant mass (a) Decay Dalitz plot for M($K\bar{K}\pi$) > 1410 MeV (b) and for M($K\bar{K}\pi$) > 1410 MeV (c) [41].

13) $\bar{p}p$ annihilation at rest in liquid hydrogen. $K\bar{K}\pi$ invariant mass with fit for the one 0^{-+} (a) and two 0^{-+} (b) hypotheses [46].

14) $\bar{p}p$ annihilation at rest in liquid hydrogen. Scatter plots of $\pi\pi\eta$ invariant mass versus recoiling $\pi\pi$ mass (a,b); $\pi\pi\eta$ invariant mass for M($\pi\pi$) < 520 MeV (insets) [49].